Visual Abstract

Delamination effect on the mechanical behavior of 3D printed polymers

F. Majid, T.Hachimi, H. Rhanim
Laboratory of Nuclear, Atomic, Molecular, Mechanical and Energetic Physics, University Chouaib Doukkali, El Jadida, Morocco
majid.f@ucd.ac.ma, http://orcid.org/0000-0001-8909-8232
Hachtaoufik@gmail.com, rhanimhassan@hotmail.com

R.Rhanim
Laboratory Study of Advanced Materials and Application, University Moulay Ismail, Meknes, Morocco
rajaaarhanim@gmail.com

ABSTRACT. This study aims to assess the delamination effect and predict the evolution of damage in 3D printed specimens to investigate the mechanical behavior occurring due to the delamination of the layers of 3D printed thermoplastic polymers. Thus, additively manufactured ABS samples are subjected to tensile tests made for different thicknesses of specimens by subtracting layer by layer.
The mechanical behavior of the layers and the adherence between the layers are studied in this paper. The deposition of the layers is modeled as a laminated material.
The delamination effect on the resistance of printed material is evaluated experimentally by comparing the mechanical characteristics of homogenously printed specimens, and laminated layers gathered together. Thus, the global resistance is reduced significantly due to the lack of adherence.
Besides, crack growth, and critical intensity factor investigation are based on damage and rupture mechanics theories.
Furthermore, the results allowed us to evaluate the energy behavior of the 3D printed material subjected to static loads and subsequently predict the evolution of the damage and find out the impact of layers delamination. Indeed, we determined three stages of damage along with the critical life fraction leading to the failure of the specimen.

KEYWORDS. Delamination, Crack growth, Printed polymers, Tensile test, Damage, ABS.

Citation: Majid, F., Hachimi, T., Rhanim, H. Rhanim, R., Delamination effect on the mechanical behavior of 3D printed polymers, Frattura ed Integrità Strutturale, 63 (2023) 26-36.

Received: 07.08.2022
Accepted: 30.09.2022
Online first: 17.10.2022
Published: 01.01.2023

Introduction

Studying industrial thermoplastic polymers is widely developed in the literature dealing with extruded ones. 3D printing has gotten more interest in the last few years, and printing technology has progressed significantly. Many studies have addressed 3D printed polymers such as PLA and ABS [1].

Many of them have been focusing on the determination of the mechanical behavior of 3D printed polymers through (i) the study of the effect of printing parameters [2], (ii) quality of the filament [3], (iii) mode I stress intensity factor [4]. Nevertheless, other barely studied aspects such as the delamination of ADM polymers, deep analysis of rupture mechanisms, and damage modeling of 3D printed ABS polymers.

The delamination effect is widely studied in composites and multilayer materials [5]. This phenomenon is recognized as a principal matter for composites, and much research has tried to deal with composites' heterogeneity and the study of the interactions between layers [6]. Additive manufacturing (ADM) of polymers has a similar concept, related to the concatenation of multiple layers according to a specific temperature, pressure, and speed [7]. In fact, the manufacturing consists of printing the specimens, through the FDM process, layer by layer with a maximum thickness of 0.2 mm until reaching the normalized one [8]. Thus, the structure of the specimens is not homogenous, and a particular phenomenon could occur in the zones between layers. The delamination effect is barely studied in ADM polymers [9], [10]. Besides, the impact of other parameters such as the density, the filling rate, and the crosshead speed on the tensile properties have been studied in different works [11].

In this paper, the delamination effect on printed material through damage and rupture mechanics has been investigated in several aspects. Indeed, this investigation has concerned three categories of additively manufactured samples. The first one concerns pre-cracked samples prepared according to the ASTM codes. The second one involves the delaminated specimens gathering separated 0.2 mm layers printed separately to construct different thicknesses. The last category concerns ADM specimens and considers subtracting one 0.2 mm layer for each life fraction, defined as the thickness variation over the normal thickness ($\Delta e/e$).

Then, the aim of damage modelling investigation is to detect the early damage that can be caused on the printed polymers, such as thickness decrease, chemical reaction, intrinsic defects due to manufacturing process or environmental effect. Thus, the failed adherence between layers or subtraction of one or more layers is modeled as a severe case of defect as those cited before. The damage modeling is realized through a modified version of the stress controlled unified theory adapted to printed material. On the one hand, the damage is given for each level of thickness, through the ratio of residual stress, the stress corresponding to the endurance limit of the material as explained by the unified theory [16]. On the other hand, an energy damage modelling is considered based on the evaluation of the area under tensile curves for each level of thickness. The obtained results had been represented in term of damage and reliability to allow us to detect the stages of the damage and to prevent accident or early failure of printed polymers.

Among many studies working over 3D printed materials, few ones address the crack growth and stress intensity factor evaluation [12]. This is one of the topics highlighted in this paper by better understanding the mechanism generated during the rupture process through the evaluation of the stress intensity factor (K_{1c}) for 3D printed materials.

Methods and materials

Fused deposition modeling

The used material is Acrylonitrile Butadiene Styrene (ABS), a rigid, heat-resistant, tough engineering plastic that is commonly used in many fields. It is an amorphous polymer composed of three monomers, Acrylonitrile, Butadiene, and Styrene [13].

The printed samples were built in our laboratory layer by layer with 3D printer machine using FDM. The setting up of the 3D printer machine is done according to the shown parameters in the Tab. 1.

Then, the machine builds the specimens in a layer-by-layer fashion. The machine's set parameters and the layer thickness determine the final product quality. For Fused Deposition Modelling, a layer thickness of 0.2 mm is typical, for Stereolithography printing can result in a quality of 0.05 – 0.1 mm. The model's size is determined by the size of the machine. During printing, the used material forms filaments, which are unwound from a coil and fed through an extrusion nozzle. The nozzle melts the filaments and extrudes them onto a built sample.

Parameter	Value
Infill density (%)	100
Feed rate (mm/s)	20 mm/s
Layer thickness (mm)	0.2
Extruder temperature (°C)	250
Bed temperature (°C)	80
Raster angles	1.2

Table 1: Extrusion parameters.

Tensile test machine

The study of printed materials such as ABS, Fig. 1, is undertaken by ISO and ASTM standards that cover all aspects, from design to failure. Indeed, the material and the experimental procedures used in this paper have been presented. The comprehension of the used experimental mechanisms is necessary for the understanding of the developed models. Therefore, two kinds of tests have been led to characterize the ABS material and evaluate the main parameter for the damage evaluation. Thus, we chose the ABS material because of its high performance and huge use in different industrial applications. Therefore, a study has been done over ADM, delaminated, and notched ABS specimens. The ADM ABS, made of many layers, subtracting one layer each time for every category of specimens, is printed in one shot by a 3D printer. The delaminated thermoplastic ABS specimens are studied through three categories of samples by considering normal samples (Cat 1), delaminated samples (Cat 2), and one-layer samples (Cat 3). For Cat 1, normal samples, it has been printed based on a fused deposition method, while for the second samples, Cat 2, artificial delamination has been considered between the three printed layers. Finally, Pre-cracked samples are Single Edge Notch Tension (SENT) specimens manufactured according to ASTM D5045 and are considered for investigating intensity factors and crack growth.
The tensile testing samples were produced per BS EN ISO 527-2:2012.

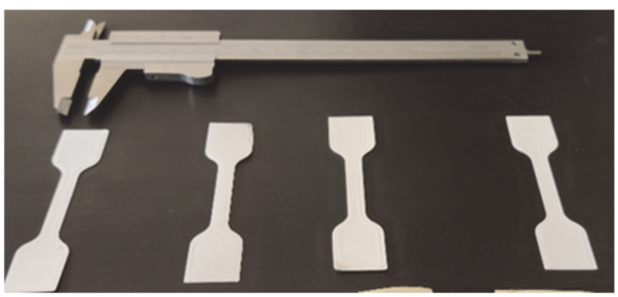

Figure 1: Delaminated Samples.

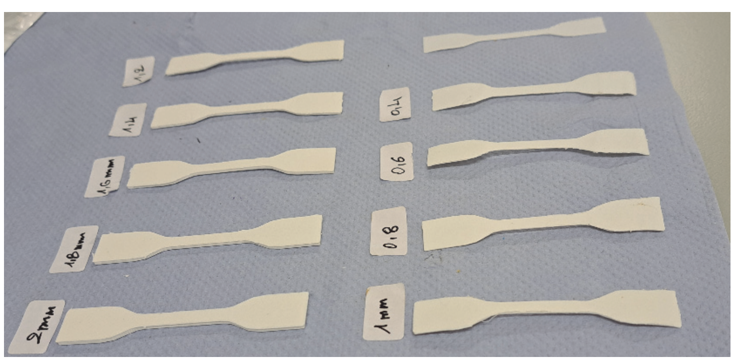

Figure 2: ABS Samples with different levels of thickness.

This study investigates the correlation between layer thickness and mechanical properties of additively manufactured parts using FDM. Therefore, mechanical tensile tests were performed on samples made of ABS filaments.

The tensile testing was performed with an MTS Tensile Testing Machine of 30 kN load cell and the crosshead speed was 1 mm/min, as shown in Fig. 3 (a).

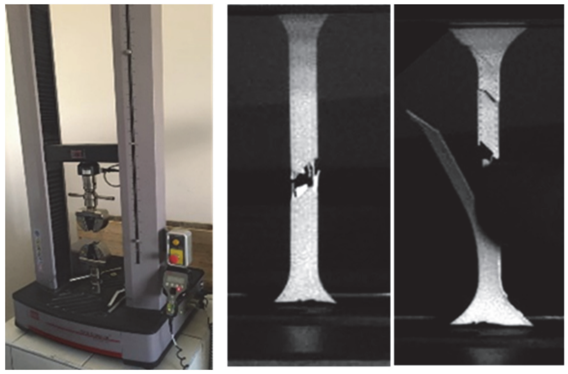

(a) (b)

Figure 3: Tensile test machine; (b) tensile test results for delaminated samples.

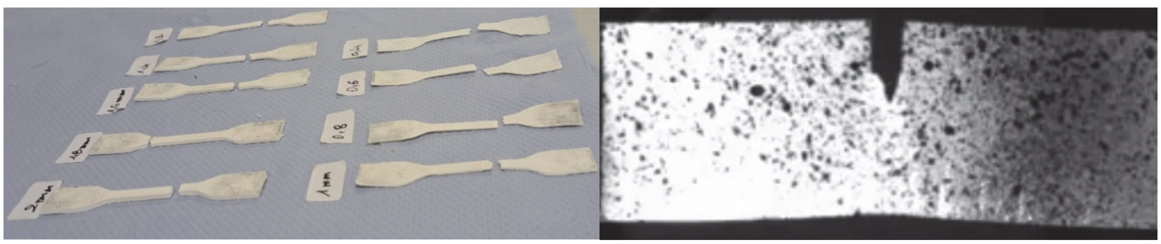

Figure 4: Tensile test results for a) ADM samples and b) SENT samples.

THEORY

Damage evaluation

The unified theory assesses the cumulative damage of materials subjected to fatigue phenomena completed by a simple static tensile test until failure. Indeed, after a predefined number of fatigue cycles, the residual endurance limit at failure is estimated at each step. In our case, a simplified approach based on variation of the thickness of printed polymers by subtracting one layer at a time is developed, considering the thickness variation as a fatigue preloading [14]. The samples are next put through tensile testing in accordance with the unified theory's principles, taking into account that thickness variation and the number of cycles used are proportional. In the next steps of this paper, the (σ, ε) curves evolutions will be considered for energy evaluation and the damage calculations based on it [16], [17].
The static damage using the stresses is expressed as follows:

$$D = \frac{1-\gamma_e}{1-\gamma_{ec}} \tag{1}$$

with: $\gamma_e = \sigma_{ur} / \sigma_u$ and $\gamma_{ec} = \sigma_a / \sigma_u$
Considering the proportionality between the energy parameter and the stresses, we obtain the static damage based on energy as shown by the Eqn. (2):

$$D = \frac{1-\gamma_e}{1-\gamma_{ec}} = \frac{1-\dfrac{U_{ur}}{U_u}}{1-\dfrac{U_a}{U_u}} \tag{2}$$

In fact, the energy damage modeling based on ultimate residual energies is represented by the variation and fluctuation of the surfaces under the (σ, ε) tensile curves as a function of time. The energy decreases with the growth of the loading level and subtraction of the supplementary layer. The tensile curves that lead directly to the estimated released energy have been used to calculate the prepared specimens' surfaces under the curve (σ, ε). Reliability and damage models were established representing the energy damage for 3D printed specimens with variable thicknesses. A comparison between the obtained model and the Miner one is detailed to analyze the represent ability of the evaluated damage.

Critical stress intensity factor

The critical stress intensity factor KIC [15], which characterizes the resistance to crack propagation, is defined according to the following formulation:

$$K_{IC} = \sigma_C \sqrt{\pi a}\, f\left(\frac{a}{W}\right) \quad (3)$$

where 'σ_C' is the critical stress, 'a' is the notch length, 'w' is the specimen width and $f\left(\frac{a}{w}\right)$ is a geometric function given by:

$$f\left(\frac{a}{w}\right) = 1.12 - 0.23\left(\frac{a}{w}\right) + 10.56\left(\frac{a}{w}\right)^2 - 21.74\left(\frac{a}{w}\right)^3 + 30.42\left(\frac{a}{w}\right)^4 \quad (4)$$

RESULT AND DISCUSSION

Delaminated samples

Fig. 5 shows the tensile test curves of the 3 categories of specimens crossing the stress and the displacement. From the curves, we notice that the mechanical behavior of the "Cat 3" (One layer) is brittle and shows a weak resistance because of the small thickness of the layer. Meanwhile, the comparison of the discrepancies between the "Cat 1" (Normal) and the "Cat 2" (Artificially delaminated) show a big difference between the two curves, and their mechanical behavior is ductile. The normal category "Cat 1" is completely fused with a very thin probability of defect between layers while the "Cat 2" have been prepared through delaminated layers, all together have the same thickness as the normal one. Those two last categories show different mechanical characteristics giving us an idea about how important adherence between the layers could be and how much the impact could be on the specimens' overall resistance.

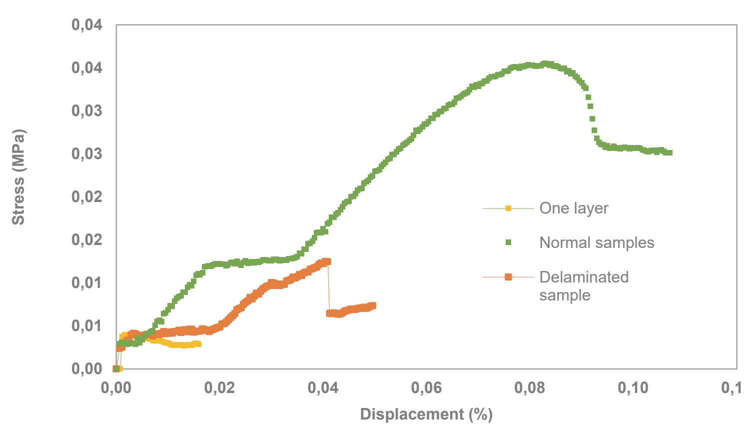

Figure 5: Tensile curves of all categories of ABS specimens.

An efficient approach has been adopted to quantify the effect of the delamination between layers through the dissipated energy allowing the rupture of the specimens. This energy is determined graphically through iterative or numerical calculations of the areas under the tensile curves of the prepared specimens, as shown in Fig. 6.

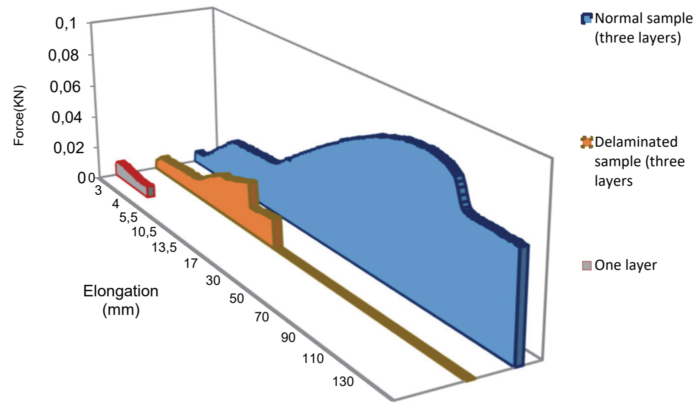

Figure 6: Calculation of equivalent energy under the surface of the tensile curves of all ABS specimens

Fig. 6 shows a significant decrease in energy from normal or ordinary manufactured specimen "Cat 1" to delaminated ones "Cat 2". Indeed, the curves of delaminated samples confirm our remarks about decreasing the mechanical characteristics of the delaminated ADM polymers while releasing a significant amount of energy because of the lousy assembly of layers.
The calculated energy for "Cat 1" is about 5.68 x 10^{-4} Joule, while the one for "Cat 2" is about 2.82 x 10^{-4} Joule. The discrepancies are quantified to be at a level of around less than 50% of energy for the delaminated specimens.

ADM samples

To consider the energy model for the ABS material, the same efficient approach, graphic iterative surface calculation, has been adopted to quantify the damage of printed ABS through the dissipated energy allowing the rupture of the specimens, as shown in Figs. 7 and 8.
A representation of the tensile curves of specimens with different levels of thickness (0.2 to 2 mm with a step of 0,2 mm) has shown that the studied specimens undergo a significant decrease in their energy corresponding to the air under the tensile curves. Indeed, this decrease is manifested by a significant reduction of the surface under the tensile curve, yield stress, and ultimate stress proportionally to the reduced number of layers, as shown in Figs. 7 and 8.
A representation of the evolution of the dissipated energy for each specimen, Fig. 9, shows a polynomial decrease that can be represented using a second-degree polynomial according to the life fraction based on the time corresponding to the ultimate residual time (t_{ur}) of the damaged specimen (Thickness loss) over the ultimate time of the normal one (t_u), $\beta_t = t_{ur}/t_u$.

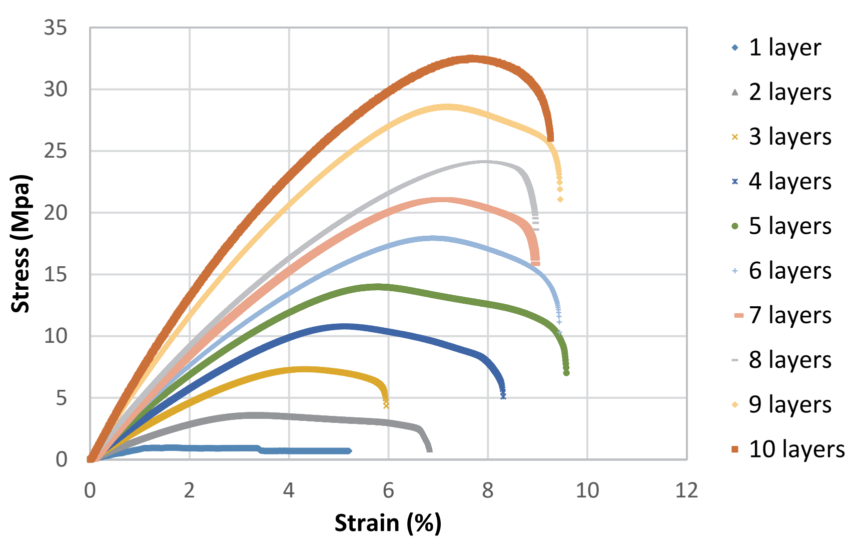

Figure 7: Tensile (σ, ε) curves of additive manufactured specimens

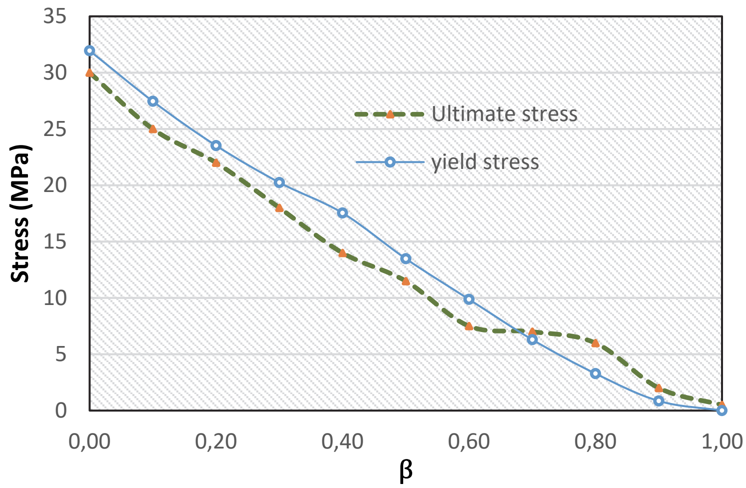

Figure 8: Yield and ultimate stresses of ADM specimens

$$y = 692.52\, x^2 - 811.75\, x + 239.29 \quad (5)$$

$$E(J) = 692.52\, \beta t^2 - 811.75\, \beta t + 239.29 \quad \text{with} \quad y = E(J)\ ,\ x = \beta_t \quad (6)$$

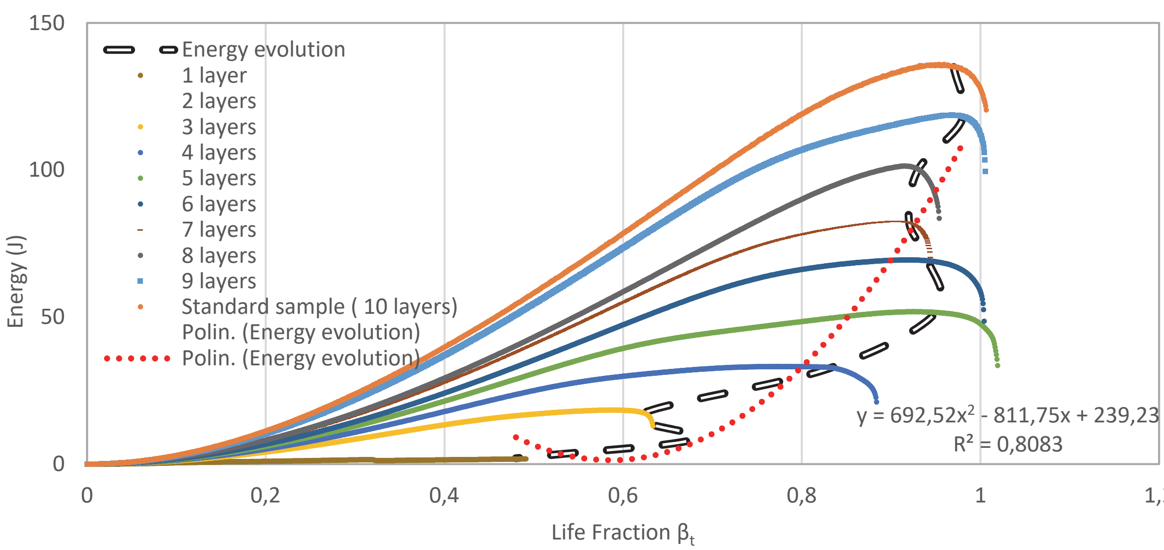

Figure 9: Maximum-recorded energy for ADM samples

The evolution of maximum energy, Fig. 10, is almost a linear trend function of the life fraction represented by the equations below:

$$y = -154.97x + 131.64 \quad (7)$$

$$E(J) = -154.97\beta + 131.64 \quad \text{with} \quad y = E(J)\ ,\ x = \beta \quad (8)$$

This evolution is linear because the maximum-recorded energy varies significantly from one specimen to another with proportional steps, as shown in Fig. 10.

Fig. 10 shows a significant decrease in energy from standard ADM ABS specimens to the most artificially delaminated ones. The evaluation of the damage occurring in the different specimens according to the models given by Eqn. (1), static damage, and presented in Eqn. (2), energy damage, compared to the Miner one, are represented in the curve of Fig. 11. They give rise to models representing the behavior of the studied specimens significantly and showing that both models are passing over the Miner damage and have the same tendency.

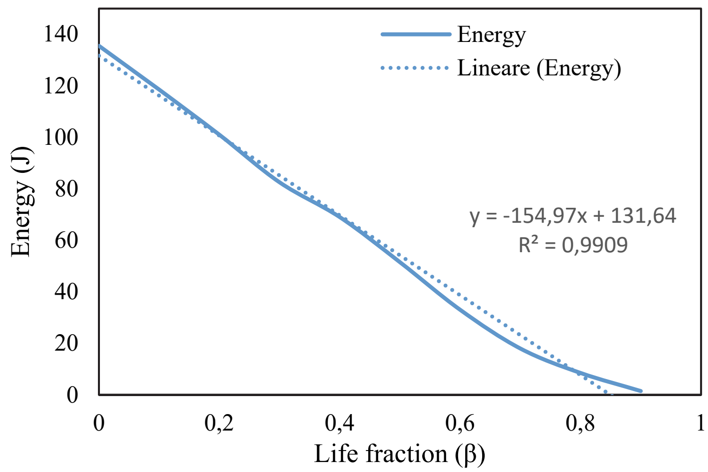

Figure 10: Maximum energy of ADM samples.

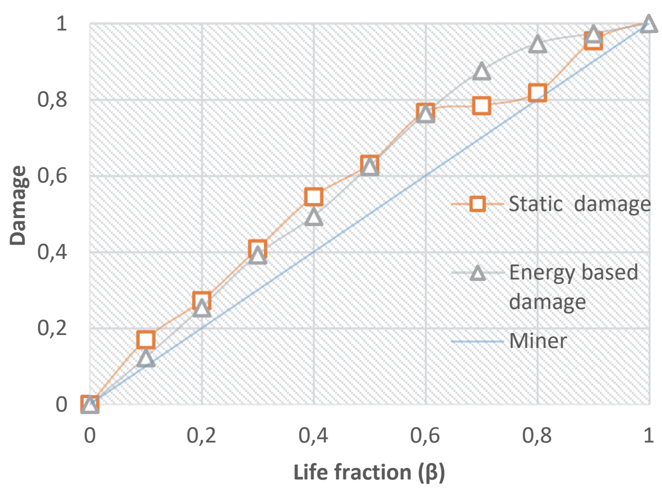

Figure 11: Tensile based on energy damage of printed ABS.

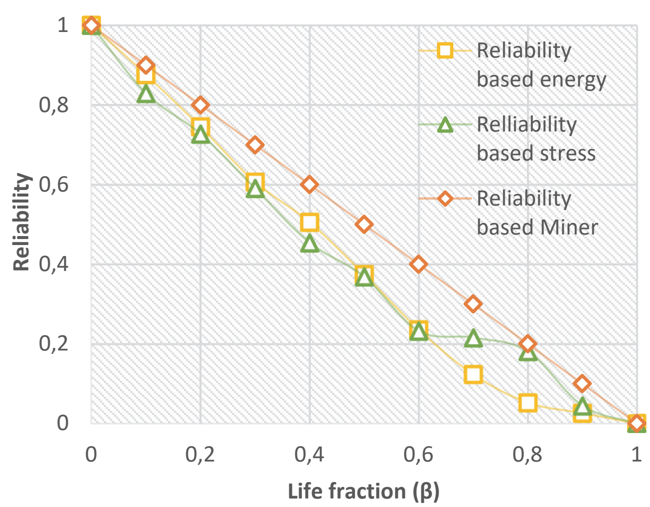

Figure 12: Comparison of the energy based on static damages.

Fig. 11 shows the evolution of the static and energy damages. It demonstrates that the 3D printed specimens of ABS polymer release a significant amount of energy noticed over the reduction of the overall resistance proportionally to the loss of thickness and subsequently to the number of delaminated layers.
By comparing the static and energy models obtained through layers' subtraction and the tensile test of the prepared specimens, we found perfect convergence between the two models, as shown in Figs. 10 and 11.
Fig. 12 shows the evolution of the specimen reliability, defined as the damage's reverse. We notice the same convergence as the damage models as much as the linearity of the models. Through the last curves, we can say that the damage is represented by a regular model of damage subdivided into three stages: Initiation [0-20%], Critical stage [20%-70%], and the accelerated stage of damage [70%-100%]. The second stage is marked by the critical life fraction βc = 50%, from which we notice a significant change in the mechanical behavior from ductile to brittle, as shown in the curves in Figs. 7and 9.

SENT samples

The results obtained for damage and rupture mechanics approaches are shown in Figs. 13 and 14.

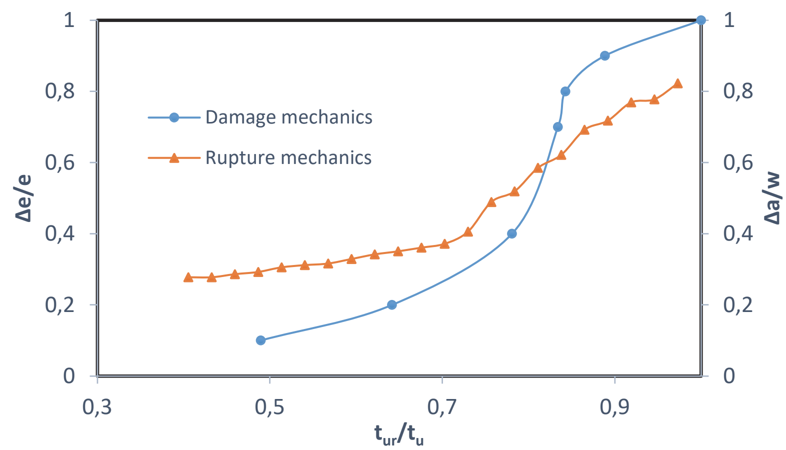

Figure 13: Crack growth based on damage and rupture mechanics approaches.

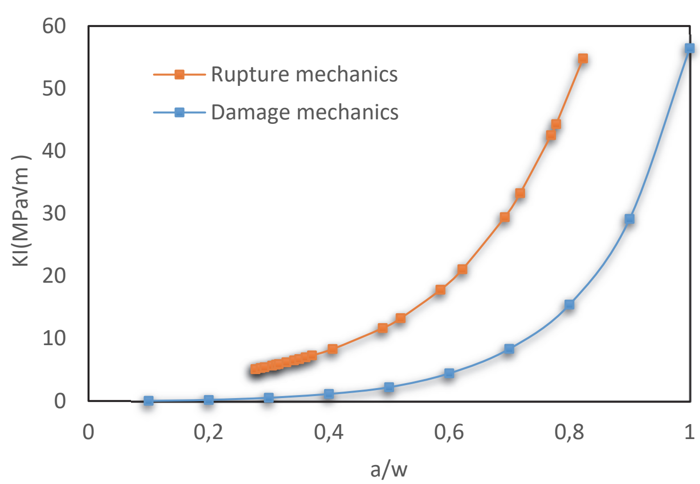

Figure 14: Stress intensity factor based on damage and rupture mechanics approaches.

From the two curves, the existence of three phases of evolution of the crack propagation speed as a function of critical stress intensity factor (FIC); in the first phase, which is characterized by an almost zero propagation speed for values of K_I lower than a threshold value of FIC. The damage of the specimen is negligible. Beyond that, the propagation velocity accelerates in a linear manner with the FIC, which is determined by K_{Ic} (Tab.2).
The stress intensity factor has been identified for the two approaches, considering the thickness fluctuation either by crack initiation or by thickness loss. Therefore, we considered the Δe similar to the Δa for the pre-cracked specimen of the third

specimen category. The comparison between the damage approach (thickness variation) and the rupture mechanics (SENT pre-crack) has shown comparable tendencies of the K_I curves. In fact, the elimination of complete layer shows an acceleration of the K_I at the third stage [70%-100%] with a weak K_{Ic}. Meanwhile the artificial SENT crack K_I evolution is engaged earlier at the second stage [20%-70%] with an important K_{Ic}. Nevertheless, the general behavior still approximatively the same considering the difference between the two approaches.

	Rupture	Damage
K_{IC} $(MPa\sqrt{m})$	5.65	1.13

Table 1: Critical stress intensity factors K_{IC}.

Conclusion

This paper examines the mechanical behavior of three categories of ABS printed specimens that have been investigated and compared under different aspects. Thus, an experimental approach has been developed to see the delamination effect of 3D printed specimens by eliminating contact between layers. The prepared categories have been tested in tensile test machines to determine the impact on the mechanical characteristics. The weakness of a single layer has been shown. The printed layer is considered as the unit of a prepared 3D printed ABS polymer, gathering and concatenating those weak layers. The adherence between those layers makes a significant difference. In fact, this difference has been proven by quantifying the energy for the tensile curves and showing that the normal specimens, which have been printed continuously, are more robust than the delaminated ones, printed separately and gathered together to simulate delamination, which have a weak adherence between layers. Therefore, the energy of the normal samples represents double of the delaminated one, which gives rise to the importance of adherence between layers even if the samples have the same thickness.

Furthermore, an energy modeling considering the maximum energy extracted from the tensile curves evolutions according to time is done to quantify the damage occurring because of delamination. We noticed that the yield stress and the ultimate stress decrease proportionally according to the reduced number of layers. In addition, the calculated energy, resulting from the multiplication of force and displacement, of tensile curves of printed ABS specimens as a function of the life fraction showed a proportional evolution because of the reduction of the surface under the tensile curve. The comparison of the static and energy damage models has shown that the obtained damages are always over the Miner one and represent the same tendencies in the two first stages, except for the third stage, which is considering an uncontrolled behavior of the material and an acceleration of the damage. The aim of our work is to prevent the infantile damage of printed polymers used in industrial applications. Therefore, the prediction of reliability parameter instead of damage parameter it necessary to decide the maintenance policy at the right time.

Finally, rupture and damage mechanics mechanisms have been investigated in the paper showing that the delamination of one layer causes approximately the equivalent damage of losing the equivalent thickness of that layer or undergoing an equivalent crack (simulated by SENT pre-crack). Presented results showed approximatively the same tendencies with a random variation at the third stage of damage [70%-100%] when the mechanical behavior accelerates, and the rupture goes straightly to the ultimate state.

Nomenclature

ABS	Acrylonitrile Butadiene Styrene
FDM	Fused Deposition Modelling
ADM	Additive Manufacturing
σ_u:	Ultimate stress
σ_a:	Just before rupture stress
σ_{ur}:	Ultimate stress at rupture
U_u:	Ultimate energy
U_{ur}:	Ultimate energy at rupture
U_a:	Just before rupture energy

γ_e	Instantaneous non-dimensional endurance limit.
γ_{ec}	Nondimensional endurance limit at failure.
D	Damage ("D = 0" for neat material, "D = 1" for completely damaged material).
$\beta= (\Delta e/e) = (n/Nf)$	Life fraction
Δe	Thickness fluctuation.

REFERENCES

[1] Majid, F., Zekeriti, N., Rhanim, R., Lahlou, M., Rhanim, H., Mrani, B. (2020). Mechanical behavior and crack propagation of ABS 3D printed specimens, Procedia Structural Integrity, 28, pp. 1719–1726. DOI: 10.1016/J.PROSTR.2020.10.147.

[2] Samykano, M., Selvamani, S.K., Kadirgama, K., Ngui, W.K., Kanagaraj, G., Sudhakar, K. (2019). Mechanical property of FDM printed ABS: influence of printing parameters, The International Journal of Advanced Manufacturing Technology 2019 102:9, 102(9), pp. 2779–2796. DOI: 10.1007/S00170-019-03313-0.

[3] Gao, X., Yu, N., Li, J. (2020). Influence of printing parameters and filament quality on structure and properties of polymer composite components used in the fields of automotive, Structure and Properties of Additive Manufactured Polymer Components, pp. 303–330. DOI: 10.1016/B978-0-12-819535-2.00010-7.

[4] Fantuzzi, N., Dimitri, R., Tornabene, F. (2016). A SFEM-based evaluation of mode-I Stress Intensity Factor in composite structures, Composite Structures, 145, pp. 162–185. DOI: 10.1016/J.COMPSTRUCT.2016.02.076.

[5] Wiener, J., Kaineder, H., Kolednik, O., Arbeiter, F. (2021). Optimization of Mechanical Properties and Damage Tolerance in Polymer-Mineral Multilayer Composites, Materials 2021, Vol. 14, Page 725, 14(4), p. 725. DOI: 10.3390/MA14040725.

[6] Zheng, S., Sun, C.T. (1998). Delamination interaction in laminated structures, Engineering Fracture Mechanics, 59(2), pp. 225–240. DOI: 10.1016/S0013-7944(97)00120-3.

[7] Woern, A.L., Byard, D.J., Oakley, R.B., Fiedler, M.J., Snabes, S.L., Pearce, J.M. (2018). Fused Particle Fabrication 3-D Printing: Recycled Materials' Optimization and Mechanical Properties, Materials 2018, 11, pp. 1413, 11(8), p. 1413. DOI: 10.3390/MA11081413.

[8] Popescu, D., Zapciu, A., Amza, C., Baciu, F., Marinescu, R. (2018). FDM process parameters influence over the mechanical properties of polymer specimens: A review, Polymer Testing, 69, pp. 157–166. DOI: 10.1016/J.POLYMERTESTING.2018.05.020.

[9] Islam, M.S., Prabhakar, P. (2017). Interlaminar strengthening of multidirectional laminates using polymer additive manufacturing, Materials & Design, 133, pp. 332–339. DOI: 10.1016/J.MATDES.2017.07.038.

[10] ASTM Committee D-30 on High Modulus Fibers and Their Composites. (1984). Effects of Defects in Composite Materials: A Symposium Sponsored by ASTM International.

[11] Hachimi, T., Naboulsi, N., Majid, F., Rhanim, R., Mrani, I., Rhanim, H. (2021). Design and manufacturing of a 3D printer filaments extruder, Procedia Structural Integrity, 33(C), pp. 907–916. DOI: 10.1016/J.PROSTR.2021.10.101.

[12] Najat, Z., Fatima, M., Rajaa, R., Ibrahim, M., Hassan, R. (2022). PVC failure modeling through experimental and digital image correlation measurements, Frattura Ed Integrità Strutturale, 16(60), pp. 488–503. DOI: 10.3221/IGF-ESIS.60.33.

[13] Araya-Calvo, M., López-Gómez, I., Chamberlain-Simon, N., León-Salazar, J.L., Guillén-Girón, T., Corrales-Cordero, J.S., Sánchez-Brenes, O. (2018). Evaluation of compressive and flexural properties of continuous fiber fabrication additive manufacturing technology, Additive Manufacturing, 22, pp. 157–164. DOI: 10.1016/J.ADDMA.2018.05.007.

[14] Majid, F., Ezzahi, M., Integrity, M.E.-P.S., 2018, undefined. (n.d.). Energy damage approaches of artificially notched and aged thermoplastic pipes, Elsevier.

[15] Zekriti, N., Rhanim, R., Majid, F., Lahlou, M., Ibrahim, M., Rhanim, H. (2020). Mode I stress intensity factors of printed and extruded specimens based on Digital Image Correlation method (DIC): Case of ABS material, Procedia Structural Integrity, 28, pp. 1745–1754. DOI: 10.1016/J.PROSTR.2020.10.149.

[16] Bui-Quoc.T, Dubuc.J, Bazergui.A, Biron.A. (1971). Cumulative fatigue damage under stress-controlled conditions, J. Basic Eng. Trans. ASME, 93, pp.691–698.

[17] Majid.F, Elghorba.M. (2017). HDPE pipes failure analysis and damage modeling. Engineering failure analysis, 71, pp. 157-165.